Journal of Environmental Radioactivity 138 (2014) 162–169

Contents lists available at ScienceDirect

Journal of Environmental Radioactivity

journal homepage: www.elsevier.com/locate/jenvrad

Optimising *in situ* gamma measurements to identify the presence of radioactive particles in land areas

Peter D. Rostron [a, *], John A. Heathcote [b], Michael H. Ramsey [a]

[a] University of Sussex, Falmer, Brighton BN1 9QG, United Kingdom
[b] Dounreay Site Restoration Limited, Dounreay, Thurso KW14 7TZ, United Kingdom

ARTICLE INFO

Article history:
Received 26 March 2014
Received in revised form
11 August 2014
Accepted 26 August 2014
Available online

Keywords:
Hot particles
Radioactive particles
Particle detection
In situ optimisation
Radioactive contamination

ABSTRACT

High-coverage *in situ* surveys with gamma detectors are the best means of identifying small hotspots of activity, such as radioactive particles, in land areas. Scanning surveys can produce rapid results, but the probabilities of obtaining false positive or false negative errors are often unknown, and they may not satisfy other criteria such as estimation of mass activity concentrations. An alternative is to use portable gamma-detectors that are set up at a series of locations in a systematic sampling pattern, where any positive measurements are subsequently followed up in order to determine the exact location, extent and nature of the target source. The preliminary survey is typically designed using settings of detector height, measurement spacing and counting time that are based on convenience, rather than using settings that have been calculated to meet requirements. This paper introduces the basis of a repeatable method of setting these parameters at the outset of a survey, for pre-defined probabilities of false positive and false negative errors in locating spatially small radioactive particles in land areas. It is shown that an un-collimated detector is more effective than a collimated detector that might typically be used in the field.

1. Introduction

A particular component of radioactive contamination in land areas is often found to be the presence of spatially small (e.g. <10 mm) particles of activity. These have been associated with various industrial processes such as releases of effluents from civil facilities (Salbu and Lind, 2005). Properly designed surveys using laboratory measurements of *ex situ* soil samples are able to provide mean activity levels within a specified area of land with defined confidence levels (USEPA, 2000). These are very likely to miss spatially small particles of activity, because of the extremely small proportion of the ground area that is investigated. If survey objectives can be satisfied by characterising the activities of gamma-emitting radionuclides, it is possible to investigate an entire survey area using gamma detection. This full coverage capability is frequently exploited in wide-area scanning surveys, for example by the Groundhog system (Dennis et al. 2007). Scanning surveys have the advantage that they are very quick to implement, and vehicle-mounted large-volume detectors are very efficient at covering open ground. The Groundhog vehicle has been shown to be capable of detecting 10^5 Bq particles at 100 mm depth with >95% probability of success at practical ground speeds (SEPA, 2005).

In circumstances where a vehicle survey is not possible, a scanning survey with portable gamma detection equipment might be used, although the probability of locating active particles is usually unknown, and is likely to be <95% (SEPA, 2005). An alternative is to set up a portable detector at a sequence of points in a systematic pattern (e.g. a regular square grid). In this type of survey, the detector height, measurement spacing and counting time are typically set by convenience (IAEA, 1998). This paper introduces a method of designing an optimised survey of this type, where the objective is to produce measurements of a quality that can enable particle detection at pre-determined probabilities of false positive and false negative errors. Example optimisations are given for ^{137}Cs contamination, using background measurements from an area of ground at the decommissioning nuclear site at Dounreay in Scotland.

1.1. Identification of a specified target source activity against a defined background

In some cases the activity of a target source that is to be found can be pre-determined. For example, the maximum activity of

* Corresponding author. Tel.: +44 1273 236593.
E-mail address: pr52@outlook.com (P.D. Rostron).

http://dx.doi.org/10.1016/j.jenvrad.2014.08.019

radioactive particles in the environment may be defined by national regulation or regulatory guidance, and more stringent requirements are often in force at specific sites in order to protect workers and to satisfy the objective of reducing risks to As Low As Reasonably Practicable (ALARP). Thus to demonstrate compliance, it may be necessary to have a low and known probability of missing a source (false negative error). However, there is the possibility that in aiming for this, a high false alarm rate (false positive error) occurs, which is time-wasting. There is therefore a potential advantage to designing surveys that enable the probabilities of false positive and false negative errors to be predetermined.

The number of counts that would be recorded by a particular detector from a known source can be calculated if the absolute detection efficiency relative to the source position and dimensions is known. The expected background counts can be estimated by direct experiment in the area of interest, or by knowledge obtained from previous experiments on substrates that are similar in their history and composition. In static measurements, both the source and background counts are directly proportional to the count duration. If the mean of the recorded background counts of successive measurements (N_{B1}) over a defined counting period (T_1) can be predicted (Fig. 1), the total counts (N_{T1}) that would be obtained if the source were present can be calculated by adding the expected source counts to N_{B1}. If, in addition, the standard deviation (σ_{B1}) of the background counts is estimated, and it is assumed that variance is proportional to $\sqrt{N}$ (using Poisson statistics), it is then possible to estimate new values of the recorded background counts (N_{B2}), recorded total counts (N_{T2}) and counting time (T_2) that would enable particle detection for defined values of false positive and false negative measurements. This adjusted counting time T_2 can be further used to derive source/detector geometries that are optimised to meet other objectives, for example the minimum overall survey time.

If the detector counts expected from a target source at counting time T_1 can be estimated (N_S), then from Fig. 1 (assuming Poisson statistics):

$$\sigma_{T1} = \frac{\sigma_{B1} \times \sqrt{N_{T1}}}{\sqrt{N_{B1}}} \tag{1}$$

where $N_{T1} = N_{B1} + N_S$. We also know that (ignoring any random or coincidence summing effects):

$$\frac{T_2}{T_1} = \frac{N_{B2}}{N_{B1}} = \frac{N_{T2}}{N_{T1}} \tag{2}$$

For the optimum scenario (Fig. 1):

$$[N_{T2} - (z_{FN} \times \sigma_{T2})] - [N_{B2} + (z_{FP} \times \sigma_{B2})] = 0 \tag{3}$$

If it is assumed that the variance is directly proportional to N ($s \propto \sqrt{N}$), then:

$$\left[N_{T2} - \left(z_{FN} \times \sigma_{T1} \times \frac{\sqrt{N_{T2}}}{\sqrt{N_{T1}}}\right)\right] - \left[N_{B2} + \left(z_{FP} \times \sigma_{B1} \times \frac{\sqrt{N_{B2}}}{\sqrt{N_{B1}}}\right)\right] = 0 \tag{4}$$

Substituting for σ_{T1} (3), and using (4) to express N_{T2} in terms of N_{B2}, this can be solved for N_{B2}:

$$N_{B2} = \left[\frac{\left(\frac{z_{FN} \times \sigma_{B1} \times \sqrt{N_{T1}}}{N_{B1}}\right) + \left(\frac{z_{FP} \times \sigma_{B1}}{\sqrt{N_{B1}}}\right)}{\left(\frac{N_{T1}}{N_{B1}} - 1\right)}\right]^2 \tag{5}$$

Finally, the adjusted counting time can be calculated:

$$T_2 = T_1 \times \frac{N_{B2}}{N_{B1}} \tag{6}$$

1.2. Application to land contaminated by small particles

The method used here for estimating the detector counts from a particle of defined activity is illustrated in Fig. 2. Given a single value of the absolute detection efficiency (ε_0) for a particle at a known position (e.g. at B) with respect to the detector at A, it is possible to estimate the absolute efficiency for a similar particle at position C (ε_1) on the ground surface by the inverse square law:

$$\varepsilon_1 = \varepsilon_0 \times \frac{AB^2}{AC^2} = \frac{h^2}{(h/\cos\theta)^2} \tag{7}$$

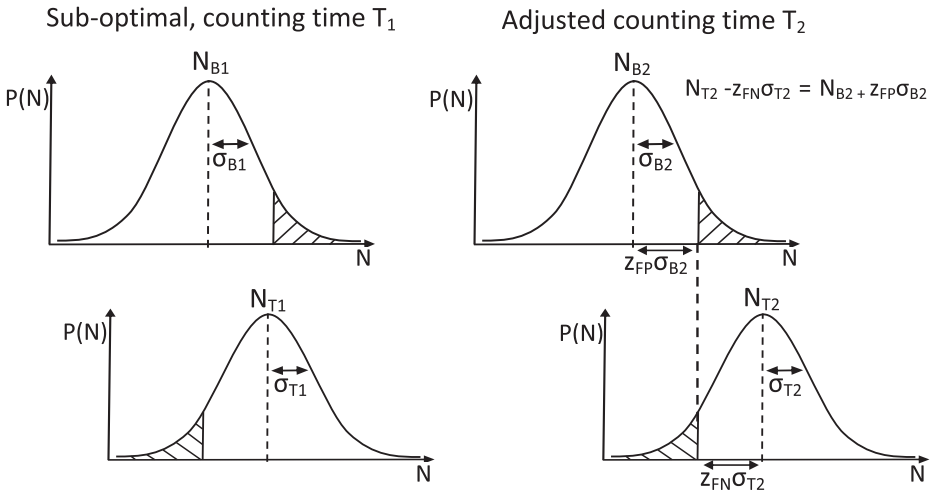

Fig. 1. The desired probabilities of false positive and false negative measurements are represented by z-scores z_{FP} and z_{FN} respectively. In the sub-optimal scenario (left) the counting time T_1 is too low for the expected total counts obtained (N_{T1}) to repeatably indicate that a source signal exists against a background distribution with mean counts = N_{B1}. In the adjusted scenario (right) the counting time has been increased to T_2, which does allow source detection at these probability levels. To achieve this, the counting time needs to be adjusted so that $N_{T2} - z_{FN}\sigma_{T2} = N_{B2} + z_{FP}\sigma_{B2}$.

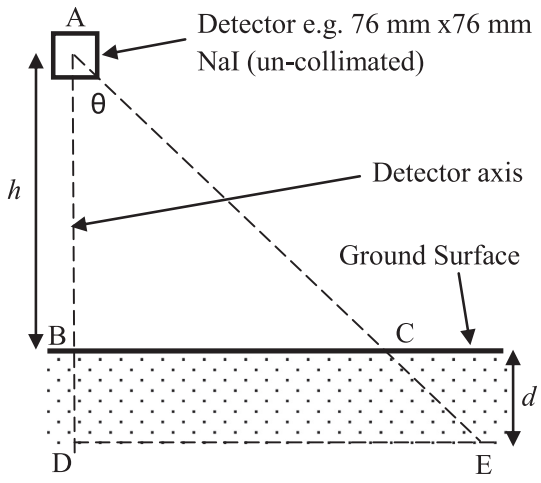

Fig. 2. Geometry of particle detection using an un-collimated NaI detector.

A Monte-Carlo methodology such as ISOCS (*in situ* Object Counting System, Canberra, 2009) can be used to estimate detection efficiencies of specific source/detector configurations. The simplified model (7) ignores effects of attenuation by air and makes the assumption that the detector volume is a sphere (with a diameter of 76 mm in Fig. 2), therefore it does not allow for different detector responses with changing θ. A NaI gamma detector which might typically be used in land investigations, and portrayed in Fig. 2, would comprise a right cylindrical volume with a length equal to its diameter. Where the distance AC is large compared to the detector volume, the spherical model is able to give reasonable predictions of absolute detection efficiencies when compared to those estimated by ISOCS for a cylindrical detector (Fig. 3), and is sufficient for the purposes of optimisation. If a detector fitted with a collimator to restrict the angle of view is used, then detector response with changing θ is complex because of the varying thicknesses of the collimator material close to the aperture. In this case, the relationship between ε_2 and ε_0 are not straightforward, and is best established by experiment, either using a calibration source or Monte-Carlo modelling.

For a buried particle at *E* (Fig. 2), attenuation by the intervening soil layer along the path length CE needs to be taken into account. Fig. 2 represents a simplified situation where the soil comprises a single layer BD with density ρ and mass attenuation coefficient μ/ρ,

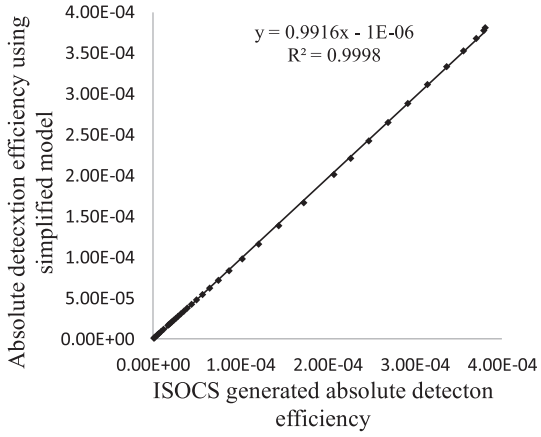

Fig. 3. Regression of absolute detection efficiencies calculated using Equation (7) against those generated by individual ISOCS geometry models for a cylindrical detector.

where μ = the linear attenuation coefficient. An approximation can be made by assuming linear attenuation of the component of emitted radiation that will contribute to the counts recorded by the detector, along the length CE. For an un-collimated detector:

$$\varepsilon_1 = \varepsilon_0 \times \frac{h^2}{((h+d)/\cos\theta)^2} \times e^{-\mu\frac{d}{\cos\theta}} \quad (8)$$

Again, this is an approximation because the actual paths of photons that potentially result in detector counts are contained within a solid angle between *E* and the total detector volume. If AE is large compared to the detector volume, then Equation (8) is a reasonable assumption to make for optimisation.

Obtaining a value for ε_0 could be achieved from first principles, providing the intrinsic efficiency of the detector is known. A practical approach would be to obtain a measured value of a calibration source, or alternatively by the creation and interpretation of a simple model using a Monte-Carlo calibration program such as ISOCS (Canberra, 2009).

2. Methods

2.1. Optimisation method

A program "Optimised Investigation of Radioactively Contaminated Land" (ROCLI) was written in Excel Visual Basic to investigate the potential for using Equations (5) and (6) in the design of particle detection surveys on contaminated land. It is intended to aid in the design of full coverage surveys and accepts the following inputs:

1. Background mean and standard deviation counts for the detector over a specified counting duration;
2. Target particle activity and depth, plus attenuation coefficient for soil (μ = 0.134 cm^{-1} in examples);
3. A range of possible detector heights *h*, (300 mm–1300 mm in steps of 100 mm used in examples);
4. A range of offsets to optimise (expressed as proportions of the detector height *h*) of the particle from the detector axis along the extended line BC (Fig. 2). These are converted by the program to offset angles (θ). Offsets of 0–10 in steps of 0.1 were used for the un-collimated scenarios described below.
5. Maximum probabilities of false positive p_{FP} & false negative p_{FN} measurements that are acceptable;
6. Total survey area (100 m^2 used in examples);
7. Measurement setup time (i.e. time between measurements, 2 min used in examples).
8. A definition of absolute detection efficiency for the target particle activity at a defined distance along the detector axis.

ROCLI assumes that a regular square-grid measurement pattern will be used in a full coverage survey. This type of systematic survey is often used in contaminated land investigations. It is known that a triangular survey pattern is geometrically more efficient at fully covering a ground area, and this could be included in future versions. Assuming that the detector response is symmetrical about its axis, the spacing between adjacent measurements for full coverage is equal to the distance between the centres of abutting coverage squares, in which the diagonal of each square is defined by the maximum circular Field-Of-View (FOV) of the detector at specific values of the detector height and offset (Fig. 4).

For each detector height and offset in the input range, ROCLI uses Equations (5) and (6) and the method outlined in Section 1.2, to calculate N_{B2} and T_2 at the defined probabilities of false positive and false negative measurements. However, if a single particle exists in the coverage square, the probability of obtaining a false

negative measurement is actually the sum of the probabilities of a false negative occurring at every point along a line perpendicular to the axis, multiplied by the respective probabilities of a randomly positioned particle existing at each of these points. ROCLI estimates this by initially calculating T_2 for the outer edge of the FOV that is defined by each height and offset (Fig. 4). It then uses T_2 to re-calculate z_{FN} (Fig. 1) for the entire coverage square. This is achieved by multiplying estimates of the probabilities of detection by the probabilities of a randomly positioned particle existing within each of 100 concentric, equally spaced annuli that are contained, wholly or partially, within the coverage square (Fig. 4). It then uses an iterative procedure to converge on the desired maximum probability of a false negative to within 0.01%. An outline flowchart is given in the Appendix.

ROCLI also calculates the number of measurements n that would be required to completely cover the survey area for each detector height and offset combination. The total survey time is calculated by multiplying n by the counting time T_2, allowing for the additional measurement setup time. The optimum scenario is considered to be the height and offset combination with the minimum total survey time, but it would also be possible to adapt this method to allow for economic factors, for example by minimising a financial loss function (Boon et al. 2007; Thompson and Fearn, 1996). Optimisation is based on single measurements, so it does not take into account the additional probability of detecting a particle located in coverage square B by adjacent measurements (e.g. A and C, Fig. 4).

2.2. Estimation of background counts

The following optimisation examples are intended for a small particle emitting radiation at 662 keV, which is a characteristic energy line of ^{137m}Ba, a short-lived daughter of ^{137}Cs. Background measurements (N_{B1}, Fig. 1) have been based on the results of a survey conducted on an unused area of ground at the Dounreay site in Scotland. Field measurements were made using a NaI 76 mm × 76 mm detector positioned at a height of 920 mm. The detector was fitted with a 90° lead collimator which had a wall thickness of 20 mm and internal aperture diameter of 25 mm. As no discernible peaks at 662 keV were observed in the target area, counts within a spectrum window 599–724 keV were used as the background measurements. This window was defined following analyses of spectra from other areas (using the same detector) that did include peaks at 662 keV. Because a collimated detector had been used, counts for the un-collimated scenario in the same area were estimated by using a Monte-Carlo application (ISOCS) to estimate the absolute efficiency of this detector at 662 keV with a source model of 100 m diameter and 0.5 m depth, making assumptions of the soil density and attenuation (Canberra, 2009). An approximation of the un-collimated background was made by generating efficiencies for both collimated and un-collimated scenarios. This is an approximation only as it does not take into account the contribution to background counts in the window arising from Compton scattering.

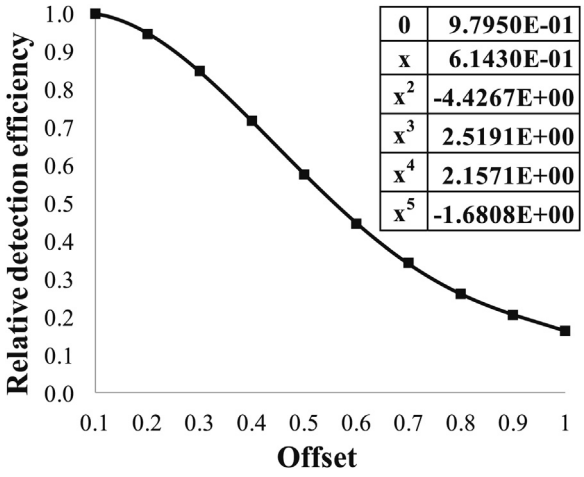

Fig. 5. Relative efficiencies of the collimated detector at different offsets. The 10 data points were generated using an ISOCS model of a 1 mm ^{137}Cs source. The apparent line joining the data points is the result of plotting efficiencies calculated by the polynomial model (inset) for 32,000 values of the offset over the full range.

2.3. Estimation of detection efficiency

For the un-collimated detector, a single value for the absolute detection efficiency of a particle emitting radiation at 662 keV was obtained using an ISOCS geometry definition of a 1 mm diameter spherical caesium particle positioned 661 mm from the lower face of the detector. As the dimensions of the detector were 76 mm × 76 mm, the actual detector-particle distance was adjusted to 661 + 76/2 = 699 mm for input into ROCLI. The optimisation then estimated absolute efficiencies for different offsets of the particle from the detector axis.

A different approach was required for optimisation with the collimator, because a collimator confers significant directional characteristics to the detector. The complex interactions between

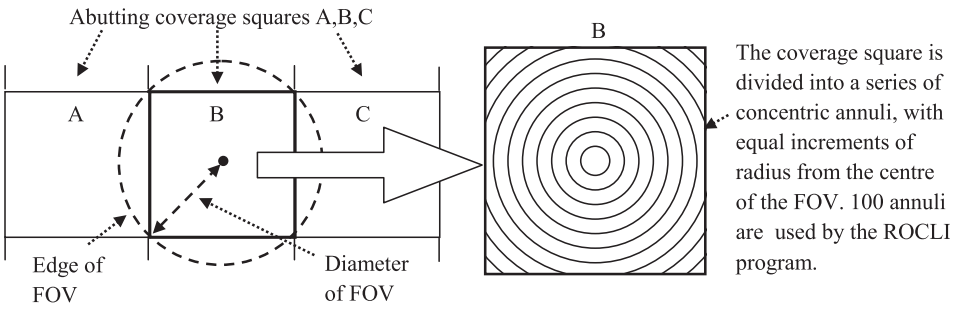

Fig. 4. ROCLI assumes full coverage will be obtained by abutting coverage squares (A, B, C) in a regular square grid. The diameter of the field-of-view (FOV) is defined by each combination of detector height and offset in the input range. Probability of a false negative for the full coverage square at a particular counting time is approximated by summing the probabilities of a false negative in each of 100 concentric annuli, taking into account the probability of a single randomly positioned particle existing in each annulus. The program then iteratively converges on the input P_{FN}.

radiation paths and the different thicknesses of lead near the collimator aperture would be extremely difficult to compute from first principles and would be different for any particular detector/collimator combination. A practical method is to model the change in angular response using a Monte-Carlo estimation of detector response at a number of different offsets. This was achieved by generating absolute detection efficiencies from ISOCS models for 10 different offsets between the detector axis and the full FOV of the collimator. A model was then created using a 5th order polynomial function (Fig. 5). High-order polynomials have potential pitfalls as they are liable to produce unpredictable results on extrapolation and interpolation. In this case, however, no extrapolation was necessary. To verify the integrity of interpolation for this particular detector/collimator combination, 32,000 equal divisions of the offset within the modelled range were generated and the function used to calculate the corresponding efficiency values. These are also plotted in Fig. 5, revealing no anomalous behaviour of the function between data points.

3. Results and discussion

The mean background count in the spectrum window was evaluated at 1696 counts for a 600 s counting time, for the collimated detector. This was converted using ISOCS to an estimate of 15,841 counts for the un-collimated scenarios. An activity level of 10^5 Bq was used for the target particle as this is the minimum activity considered to be "relevant" by the Dounreay Particles Advisory Group (DPAG, 2006). The following examples have been optimised for **minimum survey time**. Alternative detector heights and spacings could be used to give the same combinations of false positive and false negative results, but with increased overall survey times.

3.1. Example optimisations for the un-collimated detector

Four optimisations for the un-collimated detector are shown in Table 1. The probability of obtaining a false positive measurement has been fixed to $p_{FP} = 0.05$, with decreasing settings of p_{FN}. As would be expected, the optimised detector height and spacing decreases as the detection requirements become more stringent with corresponding increases in the numbers of measurements required and the total survey times. Reducing the probability of false negatives by four orders of magnitude from $p_{FN} = 0.01$ to $p_{FN} = 0.000001$ increases the overall survey time (Hours/100 m^2) but only by a factor of ~2.

The true false negative rate will in general not be known, since a missed source may never be found. However, a suitably low expected rate may be a matter of regulatory compliance. Using a value for the false positive rate (p_{FP}) = 0.05 implies that in subsequent analysis approximately 1 in 20 measurements of the background will by chance be sufficiently high that the presence of a particle could be inferred, when in fact there is no particle present. Between 2 and 5 false positive measurements would therefore be expected in the examples given in Table 1. Since positive measurements will be investigated, the false positive rate will be known. There is a potential cost in the time and money of following up false detections, However, reducing p_{FP} to 0.01 makes a relatively small difference to the number of measurements and the overall survey times (Table 2).

In a report on the management of particles at the Dounreay site up to 2005, Goss and Liddiard (2007) give an average depth of 72 mm for all the particles located over a period of 10 years. The maximum average depth in any single year was 130 mm. Table 3 shows optimisations for particles at 4 different depths increasing from 50 mm to 200 mm. As would be expected, the numbers of measurements required and the overall survey times increase significantly as particle depth increases.

3.2. Example optimisations for the collimated detector

In some circumstances a collimated detector, such as the 20 mm lead collimator used in the background measurements, might be used to reduce the effects of shine from nearby structures. Another potential use would be if the background levels in an area were totally unknown and had to be evaluated prior to optimisation. If an un-collimated detector were used in this situation, the background measurements would potentially be affected by any particles in the survey area. The use of a collimated detector would much reduce the effects that any particles had on the background measurements, providing they were not within the defined FOV of the collimator. If particles did exist within the FOV in a small number of background measurements, this would become obvious during the background survey as the affected measurements would be significantly higher than the average. Optimisations for the collimated detector at $p_{FP} = 0.05$ and for different values of p_{FN} are shown in Table 4. Comparison of these optimisations with Table 1 shows that the use of this collimator significantly increases the overall survey times when compared to the un-collimated detector.

Table 1
Optimisations for a 10^5 Bq particle at 100 mm depth, for the **un-collimated** detector and assuming Poisson variance, i.e. $\sigma^2 = N$. Calculated for $\boldsymbol{p_{FP}} = \mathbf{0.05}$ and 4 different values of p_{FN}.

ROCLI input		Optimisation				
Probability (False pos)	Probability (false neg)	Detector height (mm)	Spacing (mm)	Counting time (s)	n/100 m^2	Hours/100 m^2
0.05	0.05	800	1697	103	35	2.16
0.05	0.01	800	1471	118	46	3.06
0.05	0.0001	600	1103	107	83	5.18
0.05	0.000001	600	1018	132	96	6.76

Table 2
The optimisations shown in Table 1 with the probability of false positive measurements reduced from $p_{FP} = 0.05$ to $\boldsymbol{p_{FP}} = \mathbf{0.01}$.

ROCLI input		Optimisation				
Probability (false pos)	Probability (false neg)	Detector height (mm)	Spacing (mm)	Counting time (s)	n/100 m^2	Hours/100 m^2
0.01	0.05	800	1584	125	40	2.72
0.01	0.01	700	1386	137	52	3.72
0.01	0.0001	600	1103	142	82	5.98
0.01	0.000001	500	919	112	118	7.64

Table 3
Optimisations for a 10^5 Bq particle at 4 different depths, for the **un-collimated** detector and assuming Poisson variance. Probabilities of false measurements are $p_{FP} = 0.05$ and $p_{FN} = 0.01$.

ROCLI input	Optimisation				
Particle depth (mm)	Detector height (mm)	Spacing (mm)	Counting time (s)	n/100 m^2	Hours/100 m^2
50	1100	2489	123	16	1.09
100	800	1471	118	46	3.06
150	500	919	113	118	7.66
200	300	636	146	247	18.22

Table 4
Optimisations for the **collimated** detector, using **Poisson** uncertainty (σ = 41 counts), for particle depth = 100 mm. Calculated for $p_{FP} = 0.05$ and 4 different values of p_{FN} as in.Table 1

ROCLI input		Optimisation				
Probability (false pos)	Probability (false neg)	Detector height (mm)	Spacing (mm)	Counting time (s)	n/100 m^2	Hours/100 m^2
0.05	0.05	900	1146	121	76	5.11
0.05	0.01	900	1018	152	96	7.3
0.05	0.0001	800	792	165	159	12.64
0.05	0.000001	700	693	168	208	16.64

3.3. *Example optimisations using an empirical estimate of measurement uncertainty*

When the original survey was carried out with the collimated detector, additional measurements were recorded in order to make empirical estimates of measurement uncertainties using the Duplicate Method (Ramsey and Ellison, 2007; IAEA, 2004). Uncertainties from the duplicates were estimated by robust ANOVA (Analysis Of Variance) on an unbalanced design (Rostron and Ramsey, 2012). This apportions the total variance between large-scale spatial variation, sampling uncertainty and analytical uncertainty. The analytical uncertainty component represents the variance that would be expected if repeated measurements were acquired with the detector in the same position. At least one previous study of *in situ* measurements on land found that the precision estimated by replicated measurements was of similar magnitude to the statistical error reported for individual measurements (Golosov et al. 2000). However, there may be additional factors arising from changes in detector response during use, plus any errors in subsequent interpretation of the spectra. Optimisations using this empirical estimate of uncertainty are shown in Table 5.

The optimisation examples have been based on background counts in a spectrum window. However the method is most suited to peak area analysis in its current form. This is because the use of a linear attenuation coefficient in Equation (8) ignores the effects of Compton scattering within the soil layer. This will act to increase the counts in a spectrum window, and therefore might practically be used to infer the existence of particles using lower counting times than those predicted by the ROCLI program. ROCLI is therefore conservative in its evaluation of optimal detector height and measurement spacing for pre-defined probabilities of false results.

Table 5
The same optimisations as shown in Table 4 but using an **empirically estimated** value for the random component of analytical uncertainty (σ = 45.5 counts).

ROCLI input		Optimisation				
Probability (False pos)	Probability (false neg)	Detector height (mm)	Spacing (mm)	Counting time (s)	n/100 m^2	Hours/100 m^2
0.05	0.05	900	1146	149	76	5.7
0.05	0.01	800	905	119	122	8.12
0.05	0.0001	700	693	124	208	14.12
0.05	0.000001	700	693	207	208	18.89

This shows the effects of increasing the level of measurement uncertainty above the idealised Poisson uncertainty, to a practical level that is obtainable in the field. Overall survey times have increased by 11–14% compared to those in Table 4. Using an under-estimate of the actual uncertainty would be likely to result in increased probabilities of false positive and/or false negative measurements, thus it is recommended that empirical estimates of uncertainty are used whenever possible.

A future enhancement would be to estimate the reductions in counting times that would enable particle detection when photon scattering is taken into account.

The intention of ROCLI is to aid at the design stage of contaminated land investigations. It would be unwise to use exceedance of the value $N_{T2} - z_{FN}\sigma_{T2}$, or $N_{B2} + z_{Fp}\sigma_{B2}$ (Fig. 1) as the sole means of inferring particle existence at any one measurement location. This is because in many cases significant local variations in background levels are likely to exist within the survey area. Once a set of measurements has been obtained, inspections of individual measurements and groups of adjacent measurements are required to determine whether further action is necessary. This might be achieved by judgment or by using statistical methods such as Moran's I (Anselin, 1995). However, given pre-existing information about the expected background, ROCLI can identify settings of the detector height, measurement spacing and counting time that are likely to be able to meet the objectives of the survey with the minimum effort. It is therefore a significant advance on choosing those settings by convenience or tradition, for example the assumption that a circular area of 10 m diameter will be measured with an un-collimated detector, as has been used in some studies (Kalb et al., 2000).

The example optimisations have been made for an energy level of 662 keV, with a single value for the linear attenuation coefficient. The method could also be applied to other key-line gamma energy levels, given an adjustment to the attenuation coefficient, which is entered as a program parameter. The ROCLI program in its current form allows for 2 values of the linear attenuation coefficient to be entered for different depth ranges. The method can also be used for optimisation of surface contamination surveys (in which case there is no need to input an attenuation coefficient) which may have a potential application for post-incident response. Further practical work has also been done to investigate the assumptions made in Equation (8) (for a collimated detector) and will be reported at a later date.

4. Conclusions

A method has been devised to calculate the optimised counting time, detector height and measurement spacing required for the detection of radioactive particles at pre-defined probabilities of false positive and false negative errors, when using a static gamma detector in the presence of a known background distribution of recorded counts. This allows regulatory or similar requirements to be satisfied while controlling time-wasting false detections.

The method makes the assumption that variance is proportional to the number of counts throughout the range. It has been found that a simple geometric expression is a good match to predictions of detector response made by Monte Carlo simulation. This simple expression can be incorporated in the optimisation routine in a way that is not readily practicable for Monte Carlo calculations.

It has been demonstrated that an un-collimated detector gives better performance (less time needed for survey) than a collimated detector, despite the much lower background count rate of the latter.

Acknowledgements

The authors would like to thank the Engineering and Physical Sciences Research Council (Grant number EP/G501785/1) and the Nuclear Decommissioning Authority (under agreement number 1006695) for the joint funding of this project.

Appendix. Outline flowchart of the ROCLI program.

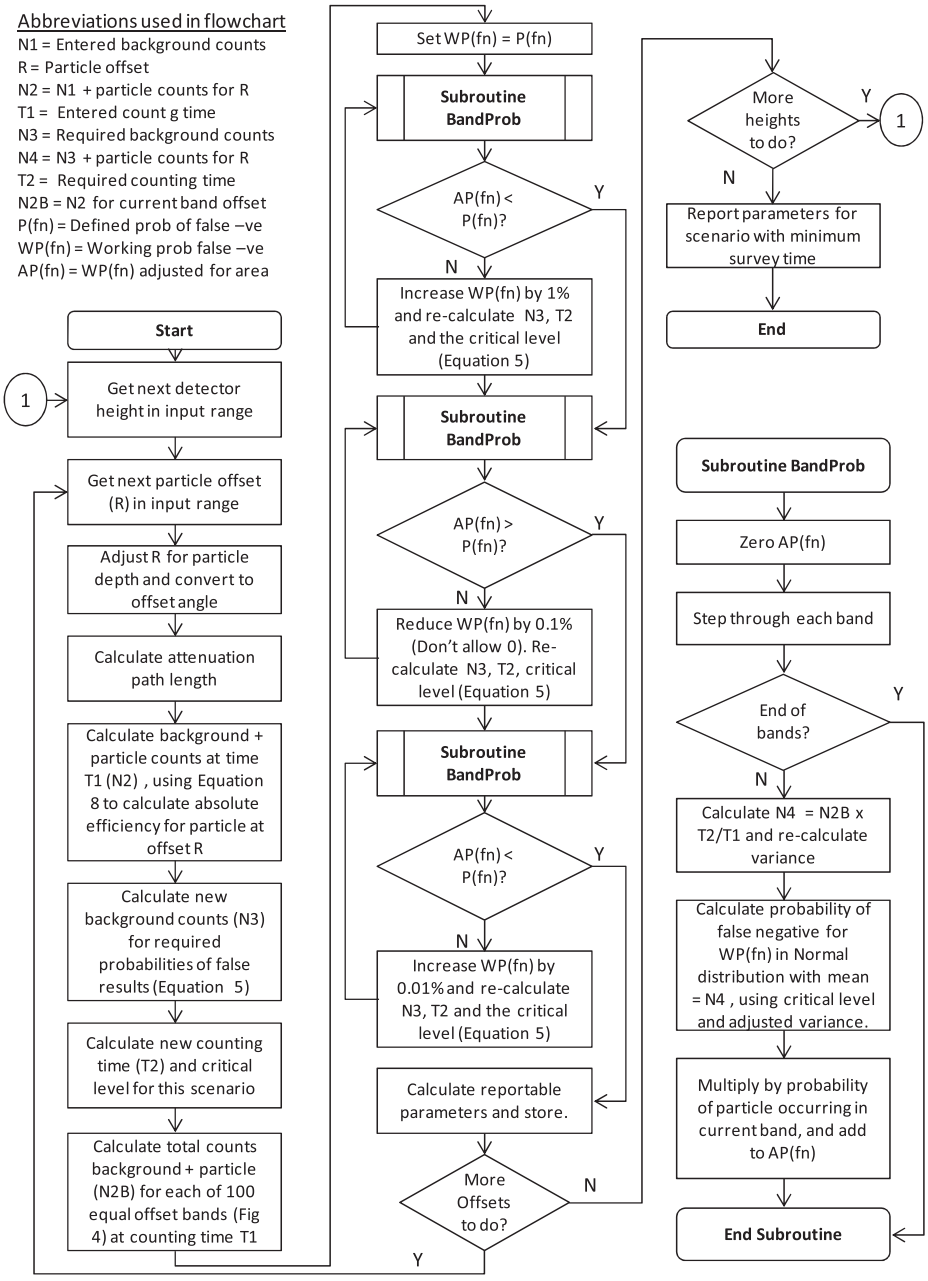

References

Anselin, L., 1995. Local Indicators of Spatial Association – LISA. Geogr. Anal. 27, 93–115.

Boon, K.A., Taylor, P.D., Ramsey, M.H., 2007. Estimating and optimising analytical and sampling uncertainty in environmental investigations: application and evaluation. Geostand. Geoanal. Res. 31, 237–249.

Canberra, 2009. ISOCS Geometry Composer Version 4.2. Canberra Industries Inc.

Dennis, F., Morgan, G., Henderson, F., 2007. Dounreay hot particles: the story so far. J. Radiological Prot. 27, A3–A11.

DPAG, 2006. Dounreay Particles Advisory Group – Third Report. SEPA.

Golosov, V.N., Walling, D.E., Kvasnikova, E.V., Stukin, E.D., Nikolaev, A.N., Panin, A.V., 2000. Application of a field-portable scintillation detector for studying the distribution of ^{137}Cs inventories in a small basin in Central Russia. J. Environ. Radioact. 48, 79–94.

Goss, O.E., Liddiard, M., 2007. Management of particles on the Dounreay site. J. Radiological Prot. 27, A89–A96.

IAEA, 1998. TECDOC-1017 Characterization of Radioactively Contaminated Sites for Remediation Purposes. International Atomic Energy Agency, Vienna.

IAEA, 2004. TECDOC-1415 Soil Sampling for Environmental Contaminants. International Atomic Energy Agency, Vienna.

Kalb, P., Luckett, L., Miller, K., Gogolak, C., Milian, L., 2000. Comparability of ISOCS Instrument in Characterization at Brookhaven National Laboratory. Brookhaven National Laboratory, New York. http://www.orau.gov/ddsc/ret/BNL-ISOCS-report.pdf.

Ramsey, M.H., Ellison, S.L.R. (Eds.), 2007. Eurachem/EUROLAB/CITAC/Nordtest/AMC Guide: Measurement Uncertainty Arising from Sampling: a Guide to Methods and Approaches. Eurachem (Eurachem Secretariat).

Rostron, P., Ramsey, M.H., 2012. Cost effective, robust estimation of measurement uncertainty from sampling using unbalanced ANOVA. Accreditation Qual. Assur. 17, 7–14.

Salbu, B., Lind, O.C., 2005. Radioactive particles released from various nuclear sources. Radioprot. Suppl. 1 (40), S27–S32.
SEPA, 2005. An Evaluation of the Sensitivity of the Groundhog Evolution™ Beach Monitoring System.
Thompson, M., Fearn, T., 1996. What exactly is fitness for purpose in analytical measurement? Analyst 121, 275–278.
USEPA, 2000. Survey Planning and Design (Chapter 5 in MARSSIM, Multi Agency Radiation Survey and Site Investigation). US Environmental Protection Agency, pp. 1–55.